

# Electrodeposition of Magnetic Films of Co-Zn in ZnCl<sub>2</sub>-DMSO<sub>2</sub>-CoCl<sub>2</sub> Molten Salt Electrolytes

Chao-Chen Yang<sup>a</sup> and Min-Fong Shu<sup>b</sup>

<sup>a</sup> Department of Environmental Resources Management, Overseas Chinese Institute of Technology, Taichung, Taiwan, R. O. C.

<sup>b</sup> Graduate School of Engineering Science and Technology (Doctoral Program), National Yunlin University of Science and Technology, Touliu, Yunlin, Taiwan, R. O. C.

Reprint requests to C.-C. Y.; Fax: 886-5-531-2071; E-mail: president@ocit.edu.tw

Z. Naturforsch. **60a**, 853 – 860 (2005); received September 10, 2005

The electrodeposition of magnetic films of Co-Zn in zinc chloride-dimethylsulfone (ZnCl<sub>2</sub>-DMSO<sub>2</sub>) molten salt electrolytes with added CoCl<sub>2</sub> has been studied. The phase diagram of ZnCl<sub>2</sub>-DMSO<sub>2</sub> molten salts was determined by differential scanning calorimetry (DSC) and thermogravimetric analysis (TGA). Various compositions of alloys with different deposition potentials on the electrode surface have been studied by cyclic voltammetry. Either the constant potential method or the pulse potential method of plating can be used for electrodepositing Co-Zn thin films. The surface morphologies and magnetic properties have been studied. It has been shown that compact needle-type Co-Zn thin films are obtained at a constant potential of  $-0.1$  V. Compact and uniform Co-Zn thin films are obtained by pulse electrodeposition. The magnetic properties of these films show higher coercive forces ( $H_c$ ) and smoother domains than those obtained by the constant potential method.

*Key words:* Pulse Potential Method; Surface Morphology; Coercive Force.

## 1. Introduction

In order to stay competitive in the near future, the electronic industry must have its magnetic material manufacturing technology moving toward larger film areas and simpler processes. The methods used so far for manufacturing thin magnetic films are operating under high vacuum and are therefore relatively costly. On the other hand, the electrodeposition method requires only simple equipment and is suitable for preparing large areas. If it can be coupled with nanotechnology of surface deposition, it will have a great potential in future magnetic film manufacturing. The pulse potential method can be operated by adjusting the  $T_{on}/T_{off}$  ratio. The advantage of this method is that, by adjusting this ratio, the size of the film granules can

be varied. In addition, nano-layer deposits of different alloy compositions can be obtained by applying different potentials. This is the main trend for the design of future electrochemical materials.

Cobalt, one of the magnetic materials, has a relatively large magnetic energy and resistance to corrosion. Thus it is an important element for manufacturing high performance memory storage magnetic media [1–5], such as magnetic-optical thin film material. Recently it has been used as the essential component for the remarkable nonvolatile magnetic random access memory.

Literature survey reveals that application of the electrodeposition method to prepare magnetic films has great potential. The one utilizing the electrochemical molten salt method for the preparation of a magnetic film, such as CoCl<sub>2</sub>-ZnCl<sub>2</sub>-BPC (butylpyridinium chloride) [6] and CoCl<sub>2</sub>-AlCl<sub>3</sub>-BPC [7] for Co-Zn, Co-Al magnetic films, is of limited use since the organic chlorides are costly, difficult to prepare and highly deliquescent. Therefore it is necessary to seek an alternative salt bath. As dimethylsulfone (DMSO<sub>2</sub>) is less deliquescent, it is an ideal stable solvent [7, 8]. This report deals with the basic physical properties of DMSO<sub>2</sub> as well as the preparation of Co-Zn magnetic

---

Abbreviations: AC, alternating current; AFM, atomic force microscopy; DC, direct current; DMSO<sub>2</sub>, dimethylsulfone; DSC, differential scanning calorimetry; EDS, energy dispersive X-ray spectroscopy;  $H_c$ , coercive force; MFM, magnetic force microscopy;  $M_r$ , remanent magnetization;  $M_s$ , saturation magnetization; RCS, refrigerated cooling system; TGA, thermogravimetric analysis; SEM, scanning electron microscopy; VSM, vibrating sample magnetometry.

films by different electrodeposition methods. By analyses of the surface properties and magnetic properties of the thin films, the feasibility of electrodepositing the magnetic film in a molten salt is assessed.

## 2. Experimental

### 2.1. Preparation of Molten Salt

ZnCl<sub>2</sub> (Merck, anhydrous, 98%) and DMSO<sub>2</sub> (Acros, 98%) were stored in a glove compartment filled with desiccated nitrogen gas. Appropriate amounts of ZnCl<sub>2</sub> and DMSO<sub>2</sub> were weighed out in the compartment. A suitable quantity of ZnCl<sub>2</sub> was slowly added to DMSO<sub>2</sub> while heating (< 70 °C), until the electrolyte became transparent. While maintaining at 70 °C, different portions of CoCl<sub>2</sub> were added to the molten salt till its concentration reached 72.8, 145.6, 218.4, and 291.2 mM and the color changed from light blue to deep blue.

### 2.2. Establishment of the Phase Diagram

The phase diagram of ZnCl<sub>2</sub>-DMSO<sub>2</sub> (Fig. 1) was obtained by measuring the decomposition temperature ( $T_c$ ) and the eutectic temperature ( $T_m$ ) by thermogravimetric analysis (TGA) and differential scanning calorimetry (DSC). To perform the TGA, 10–15 mg of molten salt were weighed in the compartment and placed in a sealed Al dish, that was then placed in a Pt dish and heated from 35 °C to 500 °C at a rate of 20 °C/min. From the temperature-related loss of weight,  $T_c$  of a molten salt can be obtained. The DSC analysis was done similarly by weighing 2–5 mg of the sample, sealing in an Al dish and heating or cool-

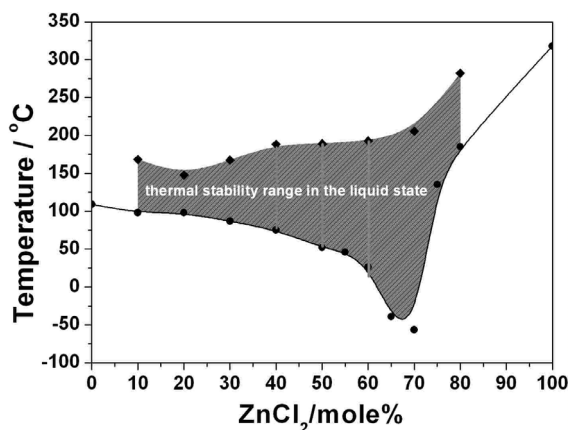


Fig. 1. The phase diagram of ZnCl<sub>2</sub>-DMSO<sub>2</sub> [8].

ing between -70 °C and 300 °C at a rate of 10 °C/min. Cooling was controlled with a refrigerated cooling system (RCS). From the relationship between the thermal function and temperature, the endothermic peak (melting curve) of the rising temperature can be obtained, and thereby  $T_m$  can be determined.

### 2.3. Determinations of the Electrical Conductivity and Density

Alternating current (AC) and direct current (DC) methods can be used for conductivity measurements. Molten salts are known for their high electrical conductivity. Therefore, in order to obtain the highest accuracy, it is better to use a relatively large electric cell compartment [9]. This compartment has a four-electrode-circuit design and is made of quartz. Pt electrodes were used. This compartment gave a cell constant of 309.88 cm<sup>-1</sup> when conducted with a KCl solution (7.42 g/1000 g of solution) at 25 °C. The density was determined by the Archimedean principle: A Pt cone immersed in the molten salt has a buoyant force equalling the displaced fluid. The Pt cone had a volume of 2.4 cm<sup>3</sup>, measured with pure water at 25 °C, whereas the diameter of the Pt thread was 0.2 mm. After it was submerged in the molten salt, an analytical balance and an auto-micro leveler were used for measuring the weight difference. By use of the Pt cone volume, the density of the molten salt can be obtained.

### 2.4. Preparation of the Electrodes

The electrochemical reactor used was a tri-electrode sealed system. All electrodes were from Nilaco Co. (99.99%). The reference electrode and the counter electrode were Zn/ZnCl<sub>4</sub><sup>2-</sup> electrodes (Zn thread, diameter: 0.8 mm). The working electrode was made of Pt (diameter: 1.5 mm), W (diameter: 1 mm) and Cu plate. All electrodes were acid washed and defatted, which was done by immersing them in a 50% HCl solution for 1–4 min and then sonicating them for 4–5 min followed by immersing in acetone. Finally these electrodes were rinsed with distilled water. The material to be electroplated was subject to fine polishing prior to the acid wash and defatting processes.

### 2.5. Constant Potential and Pulse Potential Plating

The electrodeposition methods used for the magnetic film preparation were the constant potential method and pulse potential method. The applied

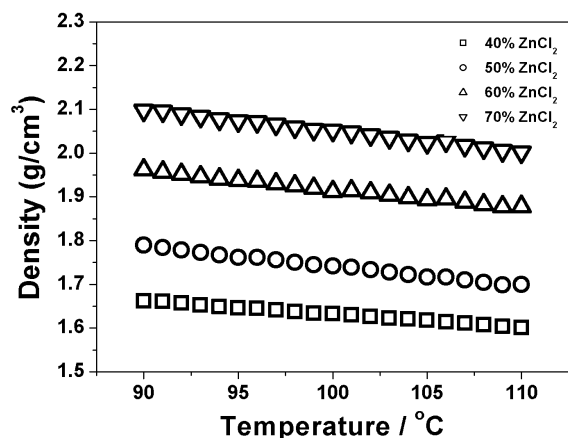


Fig. 2. The density of molten ZnCl<sub>2</sub>-DMSO<sub>2</sub> as a function of the temperature at various compositions [8].

potential was determined by cyclic voltammetry. The potential used in both methods was  $-0.1 \text{ V} \sim -0.5 \text{ V}$ , the pulse ratio  $T_{\text{on}} : T_{\text{off}} = 1 : 1$ . The surface morphologies and the magnetic properties were studied with various methods.

### 3. Results and Discussion

#### 3.1. Physical Properties of the Molten Salt

Figure 1 (i. e. Fig. 4 in [8]) shows the phase diagram of the ZnCl<sub>2</sub>-DMSO<sub>2</sub> system, derived from TG and DSC analyses. The gray area represents the thermal stability range of the liquid. The lower curve shows a minimum at 70 mol% ZnCl<sub>2</sub>. Liquids with 40, 50, 60, and 70 mol% ZnCl<sub>2</sub> were selected for conductivity and density tests. The results indicate that the density decreases slowly with increasing temperature (Fig. 2, i. e. Fig. 5 in [8]). The density also increases with increasing ZnCl<sub>2</sub> content. Essential factors affecting the molar volume and density are the formation and configuration of complex compounds [10]. The density decreased with increasing DMSO<sub>2</sub> content. It is therefore clear that addition of DMSO<sub>2</sub> favors the formation and transport of complex compounds.

The electric conductivity as a function of temperature at various compositions is shown in Fig. 3 (i. e. Fig. 7 in [8]). Conductivity increased with increasing temperature. The increase of the 60 and 70 mol% ZnCl<sub>2</sub> curves in the 60 to 85 °C range is less sharp. This is attributed to a viscosity increase, caused by the increased amount of ZnCl<sub>2</sub>. When the DMSO<sub>2</sub> content increased, the rise of the conductivity became

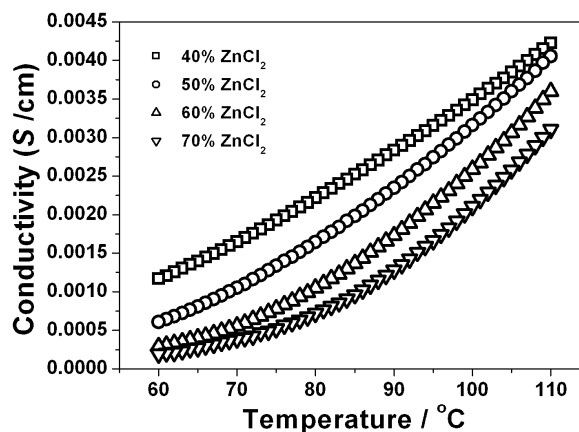
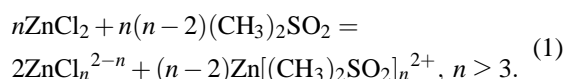


Fig. 3. The electric conductivity of molten ZnCl<sub>2</sub>-DMSO<sub>2</sub> as a function of the temperature at various compositions [8].

more prominent. For electrodeposition it is essential to choose a molten salt which has a high conductivity, so that the deposition efficiency can be maintained. For the ZnCl<sub>2</sub>-MCl binary systems, where M = Li, K, the main complex compounds are ZnCl<sup>+</sup>, ZnCl<sub>3</sub><sup>-</sup>, ZnCl<sub>4</sub><sup>2-</sup>, ZnCl<sub>6</sub><sup>4-</sup>, and ZnCl<sub>n</sub><sup>2-n</sup> [11]. Among these structures, the tetrahedral ZnCl<sub>4</sub><sup>2-</sup> has the highest stability. The equilibrium reaction of ZnCl<sub>2</sub>-DMSO<sub>2</sub> is as follows:



From this equation it is understandable that in the molten salt bath chemical species such as ZnCl<sub>n</sub><sup>2-n</sup> and Zn[(CH<sub>3</sub>)<sub>2</sub>SO<sub>2</sub>]<sub>n</sub><sup>2+</sup> complex ions exist. Besides, the coordination number of ZnCl<sub>n</sub><sup>2-n</sup> is determined by the more stable complex ion. Furthermore, the DMSO<sub>2</sub> content caused an increase in coordination number of Zn[(CH<sub>3</sub>)<sub>2</sub>SO<sub>2</sub>]<sub>n</sub><sup>2+</sup>. The results of the electrical conductivity and density clearly indicate that addition of DMSO<sub>2</sub> is advantageous for the volume increase and transition speed of complex ions.

#### 3.2. Electrode Reaction in the Molten Salt Bath

Figure 4 illustrates the voltammogram of the 50 : 50 mol% ZnCl<sub>2</sub>-DMSO<sub>2</sub> molten salt containing 0, 72.8, 145.6, 218.4, and 291.2 mM of CoCl<sub>2</sub>. It was operated with Pt as the working electrode and was scanned at 5 mV/s. The one without CoCl<sub>2</sub> showed a significant current peak when scanned at positive potential. This peak is the oxidation peak of Zn, and the positive potential limit indicates oxidation of the

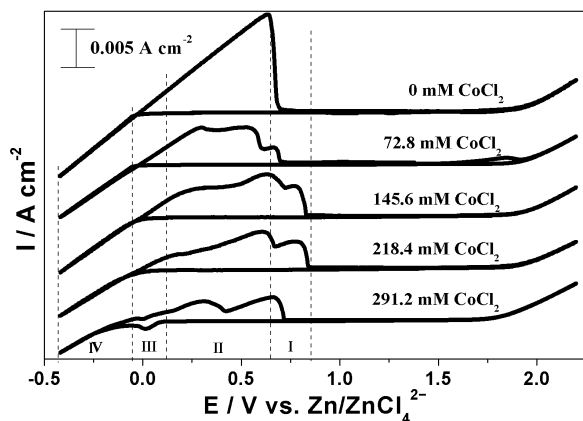
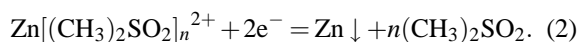
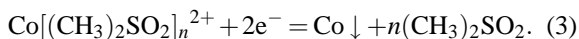


Fig. 4. Cyclic voltammograms recorded at a Pt electrode in a 50 : 50 mol% ZnCl<sub>2</sub>-DMSO<sub>2</sub> binary melt at 70 °C.

ZnCl<sub>4</sub><sup>2-</sup> complex ion to chlorine gas, whereas the negative potential limit presents the reduction peak when Zn[(CH<sub>3</sub>)<sub>2</sub>SO<sub>2</sub>]<sub>n</sub><sup>2+</sup> is reduced to Zn:



It is observed that the peak current of the Zn oxidation peak decreased with increasing CoCl<sub>2</sub> content. This is probably due to the reaction between the Co(II) ion and the Zn[(CH<sub>3</sub>)<sub>2</sub>SO<sub>2</sub>]<sub>n</sub><sup>2+</sup> complex ion, which causes the decrease of the oxidation-reduction rate of Zn. However, since Co is deposited on the Pt electrode, Co and Zn have different oxidation capabilities, and in addition, the reaction mechanism of Co and Zn codeposition is quite complicated. The Co(II) ion reacts with DMSO<sub>2</sub> and forms Co[(CH<sub>3</sub>)<sub>2</sub>SO<sub>2</sub>]<sub>n</sub><sup>2+</sup>. This ion reacts at the Pt electrode:



The above Co[(CH<sub>3</sub>)<sub>2</sub>SO<sub>2</sub>]<sub>n</sub><sup>2+</sup> ion is closely related to the oxidation-reduction reaction of Co. Hence, the main reason for the decrease of the oxidation peak of Co with increasing CoCl<sub>2</sub> content is probably due to the reaction among the Co<sup>2+</sup>, Co[(CH<sub>3</sub>)<sub>2</sub>SO<sub>2</sub>]<sub>n</sub><sup>2+</sup> and Zn[(CH<sub>3</sub>)<sub>2</sub>SO<sub>2</sub>]<sub>n</sub><sup>2+</sup> ions. In Fig. 4 the positive potential limit did not change with CoCl<sub>2</sub> content. Therefore it is very probable that the ZnCl<sub>4</sub><sup>2-</sup> and the Co<sup>2+</sup> ions did not interact. Meanwhile, when the addition of CoCl<sub>2</sub> reached 291.2 mM, there appeared a reaction peak at 0 V. In accordance with the EDS analysis on the deposition layer, this is the Co metal formed when the Co[(CH<sub>3</sub>)<sub>2</sub>SO<sub>2</sub>]<sub>n</sub><sup>2+</sup> complex ion is reduced. Therefore, when the compound deposited on the electrode surface reached a certain concentration, the reduction peak of Co can be readily observed.

### 3.3. Assessment of the Deposited Layer and Analysis of its Magnetic Properties

Magnetic films were prepared according to the information derived from the above mentioned voltammetry, i. e. applying a -0.1, -0.2, -0.3, -0.4, -0.5 V potential and a charge of 3 C. From the scanning electron microscopy (SEM) and energy dispersive X-ray spectroscopy (EDS) analyses it can be seen that when a constant potential of -0.1 V was applied, the Co content can be as high as 96 mol%. In addition, the plated layer is uniform and of needle type crystals. When a potential of -0.5 V was applied, the layer was rather compact. Layers obtained with lower deposition potential gave rise to alloy settling out [6]. The Co content in the deposited layer varied with the applied potential, and the crystals changed from needles to spheres (Fig. 5). This means that by applying different over-

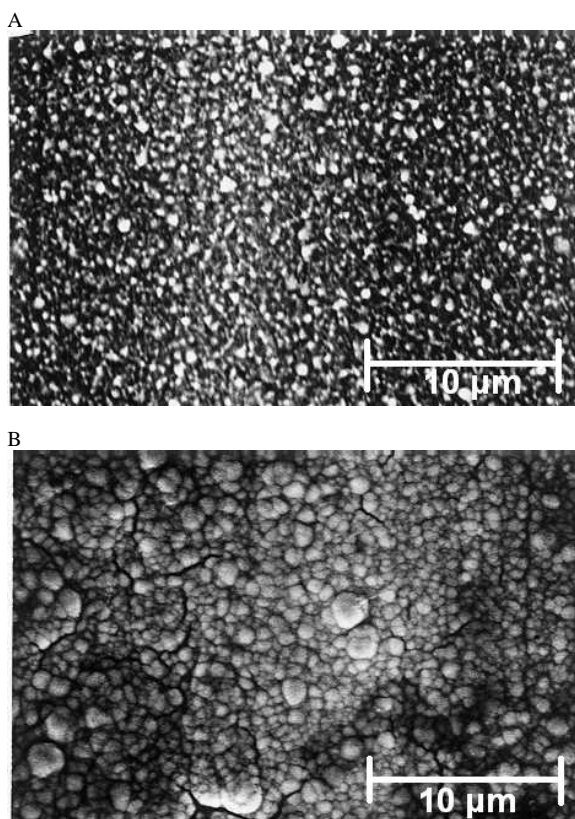


Fig. 5. Scanning electron micrographs of electrodeposited Co-Zn alloys in ternary molten salts on a Cu plate at 70 °C. Magnification is 4000×. Electrolyte: ZnCl<sub>2</sub>-DMSO<sub>2</sub>-CoCl<sub>2</sub> = 50 : 50 mol% - 291.2 mM melts. The experimental conditions: Controlled potentials A) -0.1 V, B) -0.5 V, *Q* = 3 C.

Controlled potentials	Pulse potential $T_{\text{on}}/T_{\text{off}}$	$Q$ (C)	Atomic ratio of Co:Zn Analysis of EDS	$M_s$ (memu/cm <sup>2</sup> )	$M_r$ (memu/cm <sup>2</sup> )	$M_r/M_s$	$H_c$ (Oe)
-0.1	-	3	96:4	80	43	0.53	172
-0.2	-	3	63:37	72	36	0.50	83
-0.3	-	3	30:70	73	37	0.51	88
-0.4	-	3	23:77	50	25	0.50	87
-0.5	-	3	30:70	23	86	0.37	180
-0.1	1	3	83:17	68	41	0.60	362
-0.2	1	3	59:41	75	46	0.61	195
-0.3	1	3	40:60	74	47	0.64	219
-0.4	1	3	24:76	68	42	0.62	201
-0.5	1	13:87	80	51	0.64	242	

Table 1. Electrodeposition conditions and results of Co-Zn thin films from a 50:50 mol% ZnCl<sub>2</sub>-DMSO<sub>2</sub> - 291.2 mM CoCl<sub>2</sub> melt at 70 °C.

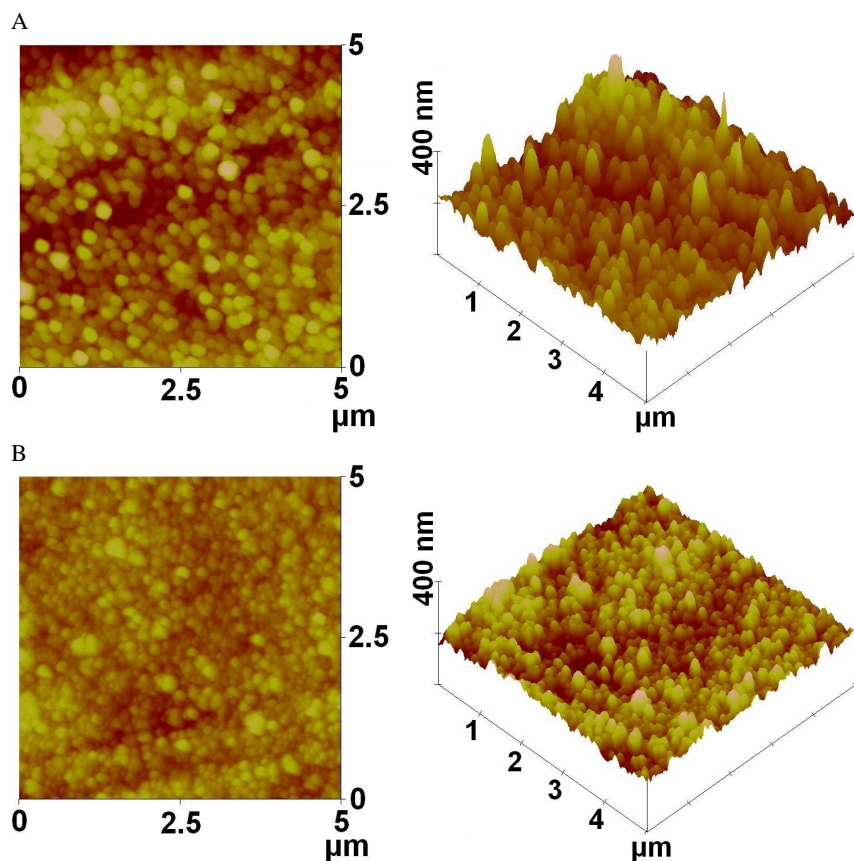


Fig. 6. Atomic force micrographs of electrodeposited Co-Zn alloys in ternary molten salts ZnCl<sub>2</sub>-DMSO<sub>2</sub>-CoCl<sub>2</sub> = 50:50 mol% - 291.2 mM on a Cu plate at 70 °C. Experimental conditions: Controlled potentials A) -0.1 V, B) -0.5 V. Pulse mode;  $T_{\text{on}}:T_{\text{off}} = 1:1$ ,  $Q = 3$  C.

potentials to the Cu electrode, the energy received by the deposited layer influences the morphology of the crystal growth. At the same electrical energy, the one with lower over-potential would need a longer deposition time. Therefore the nuclei grow mainly by diffusion. Conversely, in the situation with higher over-potential, the growth of nuclei tends to be controlled by motive power. When  $T_{\text{on}}:T_{\text{off}} = 1:1$ , unlike the constant potential method, the application of different over-potentials did not give rise to morphological dif-

ferences. Consequently, with an appropriate pulse ratio, the pulse potential deposition will produce magnetic films with different properties. Figures 6A and 6B show the atomic force micrographs when the applied potentials are -0.1 and -0.5 V. The deposited granules are of 100–300 nm size, which is near the nanoparticle size. In addition, both surfaces are uniform and compact. Therefore electrodeposition with the pulse potential method can be used for the manufacture of nano-scale magnetic films.

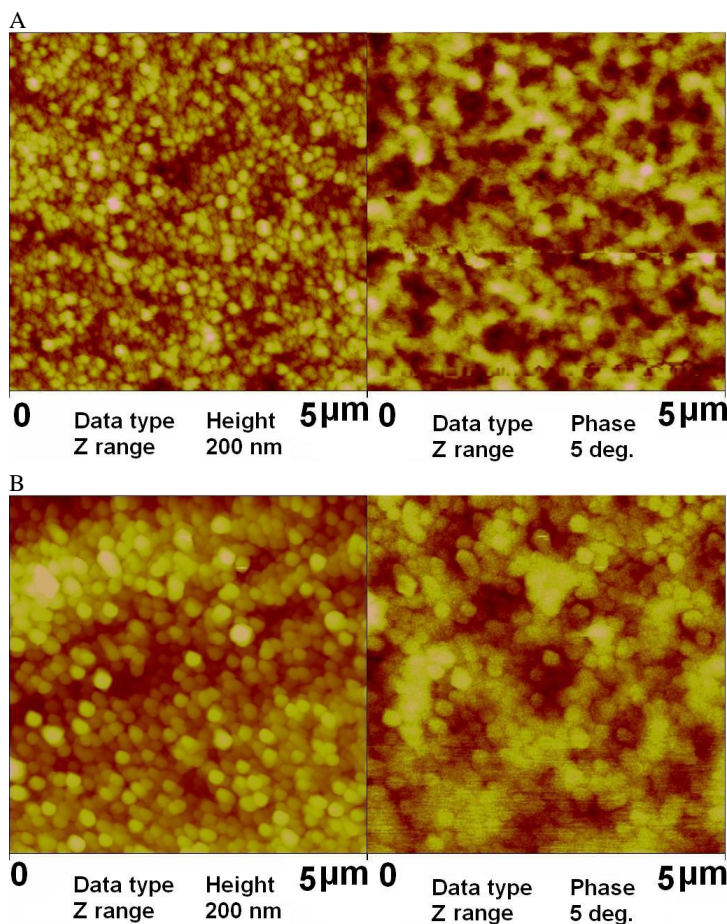


Fig. 7. Atomic force microscopy (AFM) and magnetic force microscopy (MFM) images of electrodeposited Co-Zn alloys in ternary molten salts on a Cu plate at 70 °C. Controlled potential =  $-0.1$  V; A) constant potential mode; B) pulse mode;  $T_{\text{on}} : T_{\text{off}} = 1 : 1$ .

Table 1 shows a comparison of the deposited layers, obtained by the constant potential method and the pulse potential method ( $T_{\text{on}} : T_{\text{off}} = 1 : 1$ ), where in both methods the same Coulomb electrical energy is used. The layer prepared by the pulse potential method showed a higher coercive force ( $H_c$ ) than the other layer. Factors affecting  $H_c$  are the material of the film and the affinity between the base material and the plating metal. If the deposited layer shows good adherence to the base material, its magnetization per unit area will increase. Granules of the electrodeposited layer are smaller and their compactness and adhesive force are superior to that of constant potential. On the other hand, analysis of the deposited layer with SEM, EDS and vibrating sample magnetometry (VSM) revealed that, when the Co content in the deposited layer increases, the saturation magnetization ( $M_s$ ) tends to increase too. In other words, the magnetic properties, including the coercive force ( $H_c$ ) and the remanent mag-

netization ( $M_r$ )/saturation magnetization ( $M_s$ ), of the magnetic films prepared by the pulse potential method are superior to those of the films prepared by the constant potential method. When the applied potentials are in the range of  $-0.1 \sim -0.5$  V, the  $H_c$  and  $M_r/M_s$  of the former are  $195 \sim 362$  Oe and  $0.60 \sim 0.64$ , respectively, whereas the  $H_c$  and  $M_r/M_s$  of the latter are  $83 \sim 180$  Oe and  $0.37 \sim 0.51$ , respectively. The layer prepared by the constant potential ( $-0.1$  V) method showed a higher magnetic hysteresis energy, which can possibly be attributed to increased interaction among the atoms since the deposited layer is fairly compact. The interaction causes that the magnetic moments of the atoms line up in the surface layer, which results in an increased magnetic charge, while encountering magnetization from the external magnetic field.

In magnetic physics, the magnetization in each magnetic domain is accomplished by interaction of the magnetic moments of atoms, so that magnetic spins

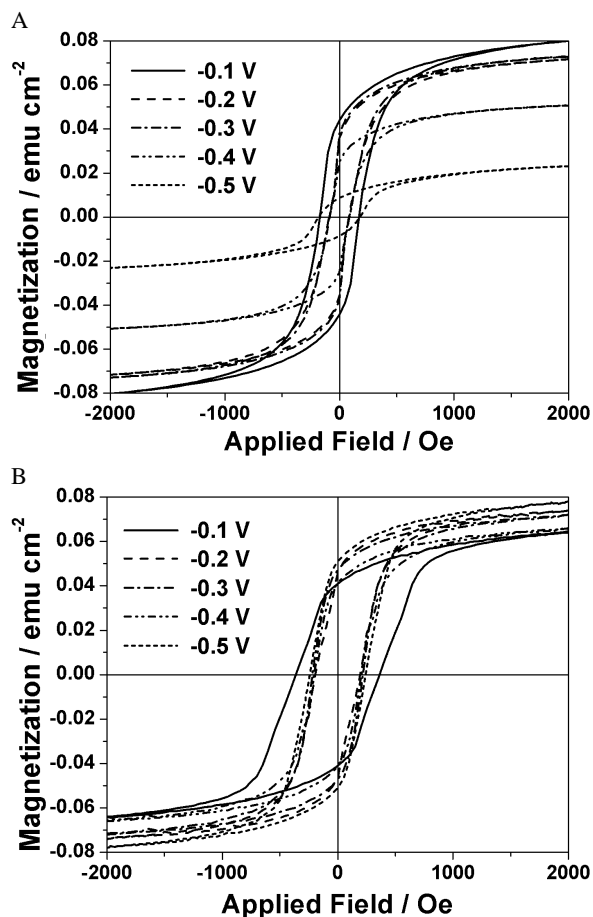


Fig. 8. Hysteresis loops of electrodeposited Co-Zn alloys on a Cu plate. Experimental conditions: A) constant potential mode; B) pulse mode;  $T_{\text{on}} : T_{\text{off}} = 1 : 1$ ;  $Q = 3$ . The layers are parallel to the magnetic fields.

align orderly. Prior to application of an external magnetic field, the spins are parallel to each other and are unidirectional and undisrupted. Domain walls, the interface of two spins of different directions, are what causes the spin to change its direction and are closely related to the continuity of the magnetic pole and the size of the magnetic domain. Magnetic force microscopy (MFM) and atomic force microscopy (AFM) results reveal that, when the magnetic hysteresis energy is high and the granules of the deposited layer are more uniform, the magnetic force will be more uniform, too, as shown in Figures 7A and 8A. Figures 8A and 8B illustrate the relation between the magnetic field intensity and the magnetized charge of the

magnetic film. From the plot, the magnetizable energy of each unit film surface, under the same magnetic field, can be determined. In addition, the size of the magnetic field needed to magnetize this film can also be obtained from this plot. The extent of its magnetization can be estimated from the shape of the loop. The squareness of the loop can be determined by the  $M_r/M_s$  value (Table 1). The total magnetizable surface energy of the magnetic film itself can be calculated from the integrated loop area. Figures 8A and 8B show the hysteresis loops of the electrodeposited films under different deposition potentials. The pulse potential method showed a larger energy of the magnetic hysteresis, which could result in an increased interaction among atoms, as the deposited layer is compacter. Besides, it causes the magnetic moments of atoms to align orderly on the surface of the deposited layer, resulting in a higher external magnetic field requirement for the overturning of the magnetic moment.

#### 4. Summary

From the experiments it is concluded that the transition rate of complex ions increases with increasing DMSO<sub>2</sub> content, and that at 40 mol% ZnCl<sub>2</sub> and 90–110 °C the most stable complex ions are formed. The reduction peak appears when the CoCl<sub>2</sub> concentration is 291.2 mM. Therefore, in order to electrodeposit a Co magnetic film, a molten salt bath having a high concentration of Co ions is preferable. Either the constant potential method or the pulse potential method can be used for the preparation of magnetic films with different Co and Zn contents. Based on the results of magnetic film analysis, the constant potential method, when applied at –0.1 V, could yield a surface with tiny and needle-shaped crystals and with higher saturated magnetization charge. In contrast, the magnetic film surface prepared with the pulse potential method has uniform and smaller granules. Also its coercive force is higher than that of the constant potential method. In summary, the use of a molten salt electrolyte and the pulse potential method can yield a magnetic film which possesses nano-particle properties.

#### Acknowledgement

The authors thank the National Science Council for financial support under the contract number NSC-90-2214-E-224-008.

- [1] C. J. Lin, J. C. Suit, and R. H. Geiss, *J. Appl. Phys.* **63**, 3835 (1988).
- [2] H. P. D. Shieh and M. H. Kryder, *J. Appl. Phys.* **61**, 1108 (1987).
- [3] J. C. A. Huang, *J. Cryst. Growth* **139**, 363 (1994).
- [4] W. Kockelmann, W. Schäfer, J. K. Yakinthos, and P. A. Kotsanidis, *J. Magn. Magn. Mat.* **177–181**, 792 (1998).
- [5] J. C. A. Huang, Y. H. Lee, Y. M. Hu, and T. C. Chang, *J. Appl. Phys.* **79**, 6267 (1996).
- [6] N. Koura, T. Endo, and Y. Idemoto, *J. Non-Cryst. Sol.* **205–207**, 650 (1996).
- [7] C. C. Yang, T. H. Wu, and M. F. Shu, *Z. Naturforsch.* **59b**, 519 (2004).
- [8] M. F. Shu, H. Y. Hsu, and C. C. Yang, *Z. Naturforsch.* **58a**, 451 (2003).
- [9] H. Y. Hsu and C. C. Yang, *Z. Naturforsch.* **56a**, 670 (2001).
- [10] D. L. Thomas, J. Y. Cherng, and D. N. Bennion, *J. Electrochem. Soc.* **135**, 2674 (1988).
- [11] R. B. Ellis, *J. Electrochem. Soc.* **113**, 485 (1966).